

# A modified laser-induced choroidal neovascularization animal model with intravitreal oxidized low-density lipoprotein

Tong Wu<sup>1</sup>, Kuan-Rong Dang<sup>1</sup>, Ya-Fen Wang<sup>1</sup>, Bao-Zhen Lyu<sup>2</sup>, Wen-Qin Xu<sup>3</sup>, Guo-Rui Dou<sup>1</sup>, Jian Zhou<sup>1</sup>, Yan-Nian Hui<sup>1</sup>, Hong-Jun Du<sup>1</sup>

<sup>1</sup>Department of Ophthalmology, Xijing Hospital, Eye Institute of Chinese PLA, Fourth Military Medical University, Xi'an 710032, Shaanxi Province, China

<sup>2</sup>Department of Anatomy and Histology and Embryology, Xi'an Health School, Xi'an 710032, Shaanxi Province, China

<sup>3</sup>The Orbital Disease Institute of the Third Medical Center of PLA General Hospital, Beijing 100039, China

**Correspondence to:** Hong-Jun Du and Yan-Nian Hui. Department of Ophthalmology, Xijing Hospital, Eye Institute of Chinese PLA, Fourth Military Medical University, Xi'an 710032, Shaanxi Province, China. dhj2020@126.com; fmmuhyn@fmmu.edu.cn

Received: 2019-12-18 Accepted: 2020-05-08

## Abstract

• **AIM:** To investigate whether intravitreal injection of oxidized low-density lipoprotein (OxLDL) can promote laser-induced choroidal neovascularization (CNV) formation in mice and the mechanism involved, thereby to develop a better animal model.

• **METHODS:** C57BL6/J mice were randomized into three groups. Immediately after CNV induction with 532 nm laser photocoagulation, 1.0  $\mu$ L of OxLDL [100  $\mu$ g/mL in phosphate-buffered saline (PBS)] was intravitreally injected, whereas PBS and the same volume low-density lipoprotein (LDL; 100  $\mu$ g/mL in PBS) were injected into the vitreous as controls. Angiogenic and inflammatory cytokines were measured by quantitative real-time polymerase chain reaction (qRT-PCR) and Western blotting (WB) after 5d, and CNV severity was analyzed by choroid flat mount and immunofluorescence staining after 1wk. *In vitro*, retinal pigment epithelial (RPE) cell line (ARPE19) were treated with OxLDL (LDL as control) for 8h. Angiogenic and inflammatory cytokine levels were measured. A specific inhibitor of lectin-like oxidized low-density lipoprotein receptor 1 (LOX1) was used to evaluate the role of LOX1 in this process.

• **RESULTS:** At 7d after intravitreal injection of 1  $\mu$ L (100  $\mu$ g/mL) OxLDL, T15-labeled OxLDL was mainly deposited around

the CNV area, and the F4/80-labeled macrophages, the CD31-labeled vascular endothelial cells number and CNV area were increased. Meanwhile, WB and qRT-PCR results showed that vascular endothelial growth factor (VEGF), CC chemokine receptor 2 (CCR2), interleukin-6 (IL-6), IL-1 $\beta$ , and matrix metalloproteinase 9 (MMP9) expressions were increased, which was supported by *in vitro* experiments in RPE cells. LOX1 inhibitors significantly reduced expressions of inflammatory factors IL-1 $\beta$  and VEGF.

• **CONCLUSION:** A modified laser-induced CNV animal model is established with intravitreal injection of 1  $\mu$ L (100  $\mu$ g/mL) of OxLDL at 7d, which at least partially through LOX1. This animal model can be used as a simple model for studying the role of OxLDL in age-related macular degeneration.

• **KEYWORDS:** age-related macular degeneration; choroidal neovascularization; oxidized low-density lipoprotein; animal model

**DOI:10.18240/ijo.2020.08.03**

**Citation:** Wu T, Dang KR, Wang YF, Lyu BZ, Xu WQ, Dou GR, Zhou J, Hui YN, Du HJ. A modified laser-induced choroidal neovascularization animal model with intravitreal oxidized low-density lipoprotein. *Int J Ophthalmol* 2020;13(8):1187-1194

## INTRODUCTION

Age-related macular degeneration (AMD) is the most common eye disease that causes blindness in the elderly<sup>[1]</sup>. According to different pathological changes, AMD can be categorized into dry (atrophic) and wet (neovascular) types, with wet AMD showing more severe effects on visual acuity<sup>[2]</sup>. The main pathological change in wet AMD is the formation of choroidal neovascularization (CNV)<sup>[3]</sup>. Therefore, elucidation of the pathogenesis of CNV is essential for treating wet AMD.

An early sign of AMD is drusen formation, which highly enriched with cholesterol, lipoproteins and polyunsaturated fatty acid phospholipids. The macular is in a high oxidative stress environment. These phospholipids are highly susceptible to oxidative stress and can be modified to oxidized phospholipids

(OxPLs)<sup>[4]</sup>. OxPLs can induce CNV formation by promoting the secretion of inflammatory and angiogenic factors from retinal pigment epithelial (RPE) cells<sup>[5-6]</sup>. Using oxidized low-density lipoproteins (OxLDL) as carriers of OxPLs, we previously demonstrated that subretinal injection of OxLDL can cause CNV-like changes. As this model brought oxidize stress into pathogenesis of CNV, it was thought to be closer to the actual situation<sup>[7-10]</sup>. However, this model shows disadvantages such as difficulty in operation, poor reproducibility, and inconvenience of CNV quantification. Therefore, it is necessary to develop a better animal model for studying the role of OxLDL in the pathogenesis of AMD. Nowadays, the most commonly used animal model of CNV is induced with laser photocoagulation by destroying the Bruch's membrane. However, this laser-induced model is created on a normal eye, it does not affect through oxidize stress. Intravitreal injection is one of the commonly used ways of intervention and is easier to perform when comparing with subretinal injection<sup>[11-14]</sup>. The study aimed to evaluate whether OxLDL intravitreal injection can enhance laser-induced CNV formation, thus to develop a new and feasible model to study the role of OxLDL in AMD.

## **MATERIALS AND METHODS**

**Ethical Approval** All animal procedures in this study were in compliance with guidelines by the Association for Research in Vision and Ophthalmology (ARVO) Statement in the use of animals research. The protocols were approved by the Institutional Animal Ethics Committee of the Fourth Military Medical University.

**Animals** Male C57BL/6J mice, aged 6-8wk and weighing 20-25 g had free access to food and water with 12h/12h light/dark cycle.

**OxLDL Injection and Laser Application** As previously described<sup>[15]</sup>, male C57BL/6J mice were anesthetized. An Iridex OcuLight GL 532 nm laser photocoagulator (Iridex) was used to create four burns with the following parameters: 120 mW power, 75  $\mu$ m spot size, and 100ms duration. The burns positions are three disk diameters away from the optic disk. Production of a bubble after the time of laser treatment is an important factor in inducing CNV; therefore, only burns in which a bubble was produced and the absence of haemorrhaging were included in this study. Next, 1.0  $\mu$ L of OxLDL [100  $\mu$ g/mL in phosphate-buffered saline (PBS)] was intravitreally injected for the experimental group, while the control group was injected with the same volume of low-density lipoprotein (LDL; 100  $\mu$ g/mL in PBS), and the blank control group was injected with the same volume of PBS.

**Evaluation of CNV Lesions** As previously described<sup>[15]</sup>, 7d after laser photocoagulation, mice were anesthetized and the chest was cut open to expose the heart. After sequential

perfusion with PBS and 4% paraformaldehyde through the heart, the eyeballs were harvested and fixed in 4% paraformaldehyde at 4°C for approximately 30min. Next, the connective tissue around the eyeball, the anterior segment and the retinal neural layer were removed under a microscope. The remaining RPE-choroid-sclera complex was immunolabeled with Isolection-IB4, Alexa Fluor™ 488 conjugate (1:100, Invitrogen, Carlsbad, CA, USA) overnight at 4°C. After washing with PBS, the choroid complex was given 4-6 radial cuts and then flat mounted on a glass slide and sealed with 50% glycerol. Images were acquired with an AX100 fluorescence microscope (Carl Zeiss, Inc., Oberkochen, Germany), and the CNV area was measured using Image J software.

**Frozen Section and Immunofluorescence Staining** Seven days after modeling, the eyeball was obtained after perfusion and fixation as described above. Then the anterior segment and vitreous were removed, and the posterior eyecups were cryoprotected in 30% sucrose solution at 4°C overnight, and then embedded and sectioned with a thickness of 10  $\mu$ m. Sections of eyeballs were washed 3 times with PBS and blocked with 1% Triton X-100 in 1% bovine serum albumin at room temperature overnight. Immunofluorescence staining was performed using the mouse monoclonal IgM antibody T15 (Sigma), the rat monoclonal IgG antibody F4/80 (Abcam), the rabbit polyclonal IgG antibody CD31 (Abcam), followed by Alexa Fluor Plus 488 rabbit anti-mouse IgM secondary antibody (Invitrogen), Alexa Fluor Plus 594 goat anti-rat IgG secondary antibody (Invitrogen), and Alexa Fluor Plus 647 goat anti-rabbit IgG secondary antibody (Invitrogen), as secondary antibodies. Then these sections were stained with DAPI (Molecular Probes, Thermo Fisher Scientific Inc., USA) and sealed with 50% glycerol. Immunofluorescence was visualized using a confocal microscope.

**Quantitative Real-time Polymerase Chain Reaction** Five days after modeling, mice were over anesthetized by intraperitoneal injection of 50 mL/kg body weight of 1% sodium pentobarbital, and eyeballs were quickly removed and choroidal tissue was obtained. Total RNA from choroidal tissue was extracted with Trizol (Invitrogen) reagent according to the manufacturer's instructions. Complementary DNA (cDNA) was synthesized using a cDNA Synthesis Kit (TaKaRa, Japan), and PCR amplification was conducted using SYBR® Green PCR Master Mix Reagent (TaKaRa, Shiga, Japan) on the ABI PRISM Step One Plus real time PCR system (Applied Biosystems, Foster City, CA, USA). The mRNA expression was normalized to that of the endogenous reference gene  $\beta$ -actin. The primer sequences are listed in Table 1.

**ARPE19 Cell Culture and Treatment** The human RPE cell line ARPE19 was purchased from the Chinese Academy of Sciences cell bank and was routinely cultured in low-

**Table 1 Primers used in qRT-PCR**

Gene	Forward primer (5'-3')	Reverse primer (5'-3')
β-actin	CATCCGTAAAGACCTCTATGCCAAC	ATGGAGCCACCGATCCACA
IL-6	TAGTCCTTCTACCCCAATTTCC	TTGGTCCTTAGCCACTCCTTC
IL-1β	GCAACTGTTCTGAACCTCAACT	ATCTTTTGGGGTCCGTCAACT
CCR2	ATCCACGGCATACTATCAACATC	CAAGGCTCACCATCATCGTAG
MMP9	CTGGACAGCCAGACACTAAAG	CTCGCGGCAAGTCTTCAGAG
LOX1	CAAGATGAAGCCTGCGAATGA	ACCTGGCGTAATTGTGTCCAC

qRT-PCR: Quantitative real-time polymerase chain reaction.

**Table 2 Primary antibodies used in WB**

Antibody	Host species	Concentrations	Catalog number	Company
β-actin	Mouse	1:2000	#3700	CST, American
β-tubulin	Rabbit	1:2000	#2148	CST, American
GAPDH	Rabbit	1:2000	#5174	CST, American
IL-1β	Rabbit	1:1000	ab9722	Abcam, American
IL-6	Rabbit	1:1000	ab6672	Abcam, American
CCR2	Rabbit	1:1000	ab203128	Abcam, American
VEGFA	Rabbit	1:1000	ab46154	Abcam, American
T15 (IgM)	Mouse	1:1000	330001	Avanti Lipids, American
MMP9	Rabbit	1:1000	#13667	CST, American
LOX1	Rabbit	1:1000	ab60178	Abcam, American
F4/80	Rat	1:1000	ab6640	Abcam, American

WB: Western blotting; IL: Interleukin; CCR2: CC chemokine receptor 2; VEGFA: Vascular endothelial growth factor-A; MMP9: Matrix metalloproteinase 9; LOX1: Lectin-like oxidized low-density lipoprotein receptor 1.

glucose DMEM medium containing 10% fetal bovine serum in a humidified environment of 5% CO<sub>2</sub> at 37°C. The cultured ARPE19 cell was divided into 3 groups, and 25 μg/mL OxLDL was treated for the experimental group, while the control group was treated with 25 μg/mL LDL, and the blank control group was added with the same concentration of PBS.

**Western Blotting** Tissues were harvested 5d after modeling, and ARPE19 cells were harvested at 8h after treatment. Proteins were extracted using cell lysis buffer supplemented with proteinase and phosphatase inhibitors, and protein concentration was determined by BCA protein assay kit (Sangon Biotech, Shanghai, China). Equal amounts (20 μg) of protein were separated by SDS-PAGE and transferred to polyvinylidene fluoride membranes (Millipore, Billerica, MA, USA). After blocking in 5% skim milk for 2h at room temperature, the samples were incubated overnight at 4°C with primary antibodies (Table 2). After washing three times with TBST, the samples were incubated 1h at room temperature with the secondary antibody. Bound antibodies were and visualized by enhanced chemiluminescence reagents ECL (Pierce, Rockford, IL, USA).

**Statistical Analysis** Statistical analysis was performed using SPSS 22.0 software (SPSS, Inc., Chicago, IL, USA). Data between two groups were compared using Student's *t*-test; one-way ANOVA was used to compare multiple sample means,

and LSD-*t* test was used for comparison between groups. All analyses and graphic representations were performed using GraphPad Prism software (version 4.0c; GraphPad, Inc., La Jolla, CA, USA). Values are represented as the mean±standard error of the mean (SEM). *P* values of less than 0.05 were considered as significant.

## RESULTS

**Intravitreal Injection of OxLDL Promotes Laser-induced CNV Formation** First, we evaluated the effects of OxLDL and LDL on CNV formation *in vivo*. Flat mount staining showed that CNV area after 7d of the OxLDL group was significantly larger than that of the LDL and control groups (OxLDL 48 256.13±14 480.49 μm<sup>2</sup>, LDL 28 490.7±9095.84 μm<sup>2</sup>, control 25 936.4±8358.05 μm<sup>2</sup>; *P*<0.05, *n*=12; Figure 1). These results suggest that intravitreal injection of OxLDL can significantly promote laser-induced CNV, whereas LDL and PBS does not.

**OxLDL Promotes Macrophage Aggregation and VEGF Expression in CNV Lesions** Immunofluorescence staining was performed with CD31, T15, and F4/80 as markers of vascular endothelial cells, OxLDL, and macrophages, respectively. OxLDL was deposited around the CNV, consistent with F4/80-positive macrophage localization (Figure 2A, 2B). The expression of vascular endothelial growth factor (VEGF) in the choroidal tissue of the OxLDL group was significantly

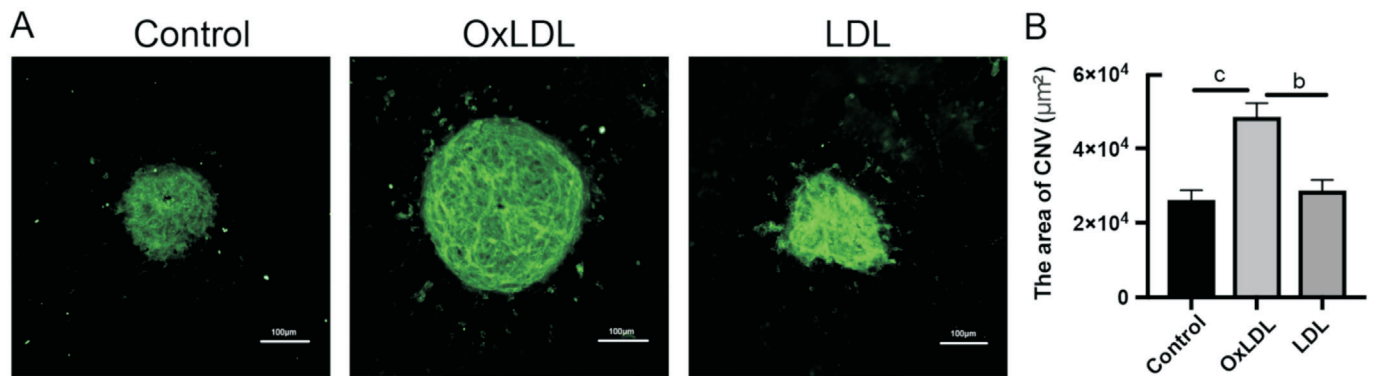


**Figure 1 OxLDL promoted laser-induced CNV in mice** A: Representative images of CNV in different groups. Blood vessels in choroidal flatmounts were stained with Alexa Fluor™ 488 conjugate Isolectin-IB4. B: The quantification result of CNV area. Data are mean±SEM. <sup>b</sup>*P*<0.01, <sup>c</sup>*P*<0.001.

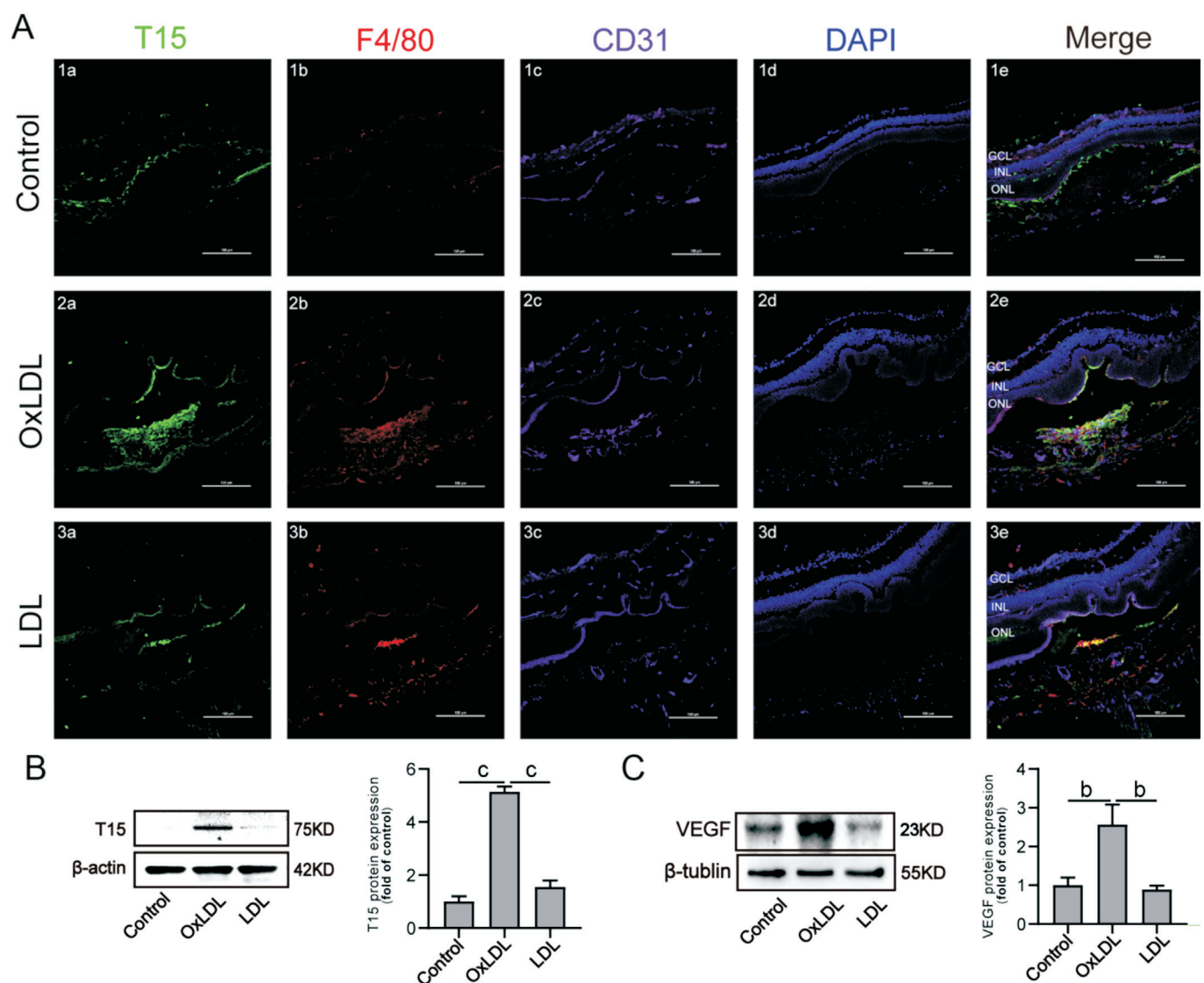


**Figure 2 OxLDL promotes macrophage aggregation and VEGF expression in CNV lesions** A: Immunofluorescence staining: T15 mark OxLDL, F4/80 mark macrophages, CD31 mark vascular endothelial cells, and DAPI; B: Representative WB analysis and quantification of relative expression of T15. Data are mean±SEM. <sup>c</sup>*P*<0.001. C: Representative Western blot analysis and quantification of relative expression of VEGF. Data are mean±SEM. <sup>b</sup>*P*<0.01.

higher than that of the LDL and control groups (Figure 2C). OxLDL diffuses from the damaged retina to subretinal and

around CNV area, promotes macrophage aggregation and VEGF expression, thereby promoting CNV formation.

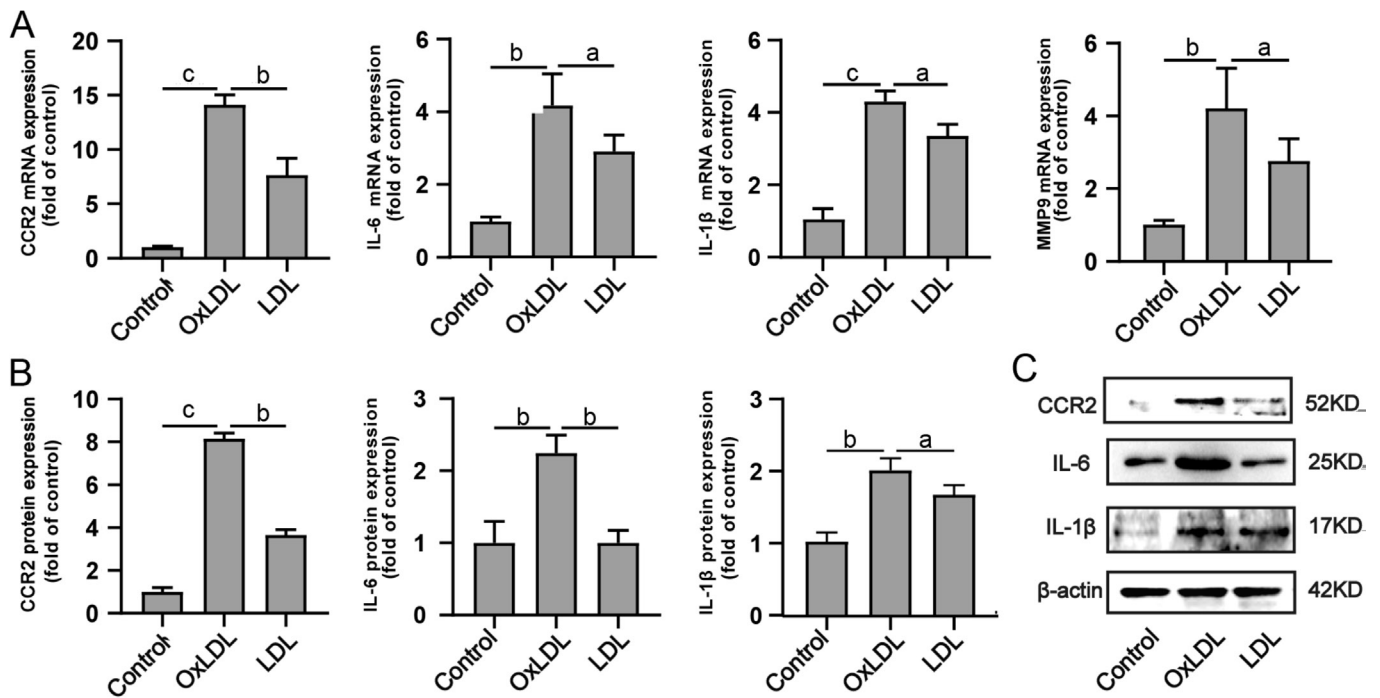


**Figure 3 OxLDL promotes expression of inflammatory cytokine secretion** A: qRT-PCR assay analyzed some of the angiogenic factors; B: Quantification of relative expression of CCR2, IL-6 and IL-1β. Data are mean±SEM. <sup>a</sup>*P*<0.05, <sup>b</sup>*P*<0.01, <sup>c</sup>*P*<0.001. C: Representative WB analysis of CCR2, IL-6 and IL-1β.

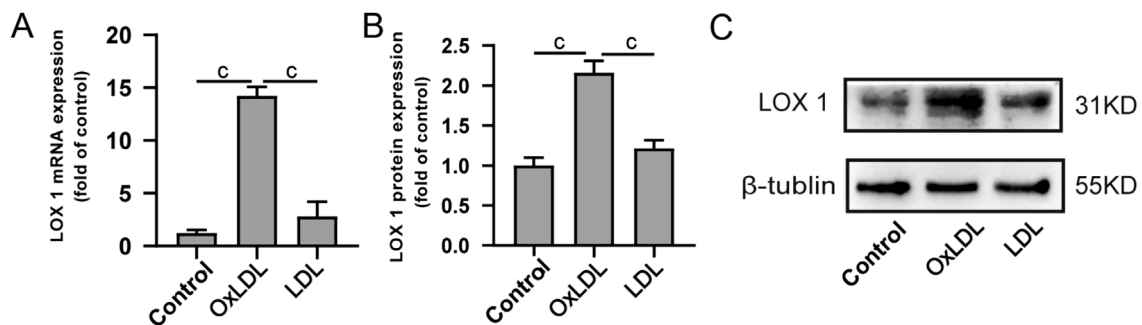


**Figure 4 OxLDL promotes the expression of its receptor LOX1** A: qRT-PCR assay analyzed LOX1; B: Quantification of relative expression of LOX1. Data are mean±SEM. <sup>c</sup>*P*<0.001. C: Representative WB analysis of LOX1.

**Vitreous Injection of OxLDL Promotes Inflammatory Cytokine Secretion** The quantitative real-time polymerase chain reaction (qRT-PCR) results showed that the mRNA levels of CC chemokine receptor 2 (CCR2), interleukin-1β (IL-1β), IL-6, and matrix metalloproteinase 9 (MMP9), in the choroidal tissues of the OxLDL and LDL groups were up-regulated and higher than those in the control group. Cytokine levels in the OxLDL group were higher than those in the LDL group (Figure 3A). Western blotting (WB) showed that the protein expression of CCR2, IL-6, and IL-1β in the OxLDL and LDL groups was higher than that in the control group, and the expression in the OxLDL group showed a more obvious increase (Figure 3B, 3C).

**OxLDL Promotes the Expression of its Receptor LOX1 in Choroidal** To study the mechanism of OxLDL, we further evaluated the effect of OxLDL on the expression of

lectin-like oxidized low-density lipoprotein receptor 1 (LOX1), which is the main receptor of OxLDL. The results of qRT-PCR and WB showed that OxLDL significantly promoted the expression of LOX1, while LDL had no such effect (Figure 4). **OxLDL Promotes LOX1, VEGF, IL-6, and IL-1β Expression of RPE Cells** We investigated the expression changes of inflammatory and angiogenic factors after treated by OxLDL. The experiment demonstrated that OxLDL promotes the expression of VEGF, IL-6, and IL-1β in ARPE19 cells. We further observed the effect of OxLDL on its receptor's expression and found that LOX1 was activated in a dose-dependent manner (Figure 5).

**OxLDL Regulates the Cytokines Expression Through LOX1** Our experiments showed that OxLDL promotes the expression of inflammatory factors expression. However, whether the inflammatory factor expression is LOX1

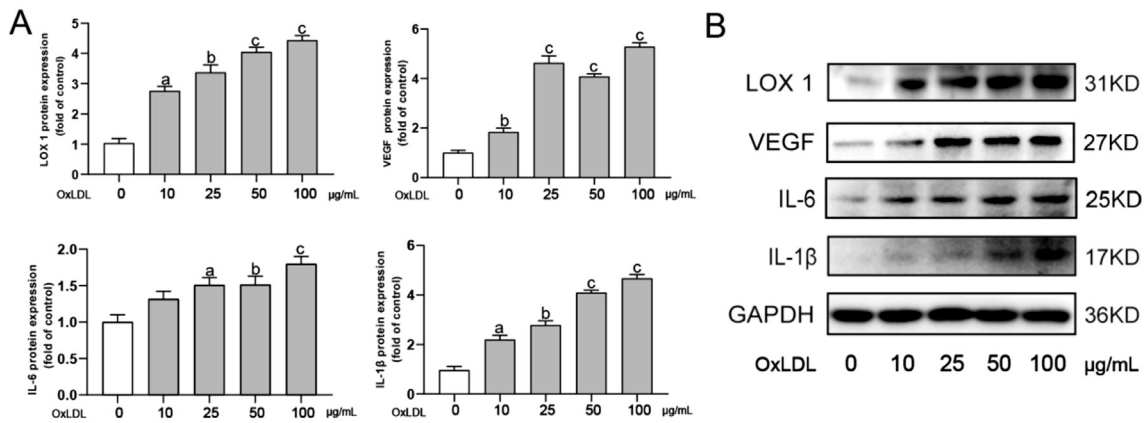


**Figure 5 OxLDL promotes expression of LOX1, VEGF, IL-6, and IL-1β** A: Quantification of relative expression of LOX1, VEGF, IL-6, IL-1β. Data are mean±SEM. <sup>a</sup> $P < 0.05$ , <sup>b</sup> $P < 0.01$ , <sup>c</sup> $P < 0.001$ . B: Representative WB analysis of LOX1, VEGF, IL-6, IL-1β.

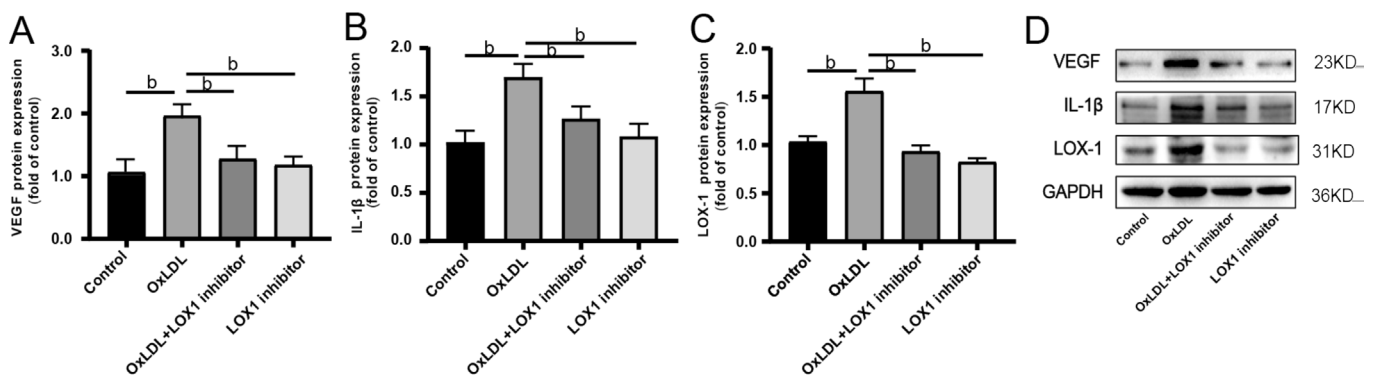


**Figure 6 OxLDL regulates the cytokines expression through LOX1** A-C: Quantification of relative expression of MMP9, IL-1β and LOX1. Data are mean±SEM. <sup>b</sup> $P < 0.01$ . D: Representative WB analysis of VEGF, IL-1β and LOX1.

dependent was not clear. Thus, we added LOX1 inhibitor to the culture medium and then observed the effect of OxLDL on the expression of inflammatory factors. WB analysis showed that the expression of IL-1β and VEGF was decreased when the expression of LOX1 was inhibited (Figure 6).

**DISCUSSION**

OxLDL can cause disorders of lipid metabolism, and in addition it can cause an inflammatory response, further promoting pathological angiogenesis<sup>[16-17]</sup>. OxLDL induces the accumulation of reactive oxygen species (ROS) intracellular and promotes inflammatory responses, and there is evidence that high concentrations can lead to apoptosis of cells<sup>[18]</sup>. There are many studies have shown that OxLDL to be associated with the incidence of retinopathy and other diseases. OxLDL leads to increased oxidative stress and vascular endothelial cell dysfunction *via* interaction with a cell surface scavenger receptor, CD36<sup>[19]</sup>. Study in diabetic retinopathy demonstrated OxLDL causes increased oxidative stress, increased VEGF expression, and apoptosis, causing retinal damage<sup>[20]</sup>. In the study of AMD, it is confirmed that OxLDL is a major component of drusen, which promotes CNV formation of wet-AMD, but the specific mechanism has not proved yet<sup>[21]</sup>. While the detailed mechanism of CNV and how to control it

remained to be revealed, an ideal animal model is needed. The laser-induced CNV model is now the most commonly used model, in which the laser directly damages the choroid-Bruch’s membrane-RPE complex, choroid tissue then fills the wound and expands into the subretinal cavity<sup>[11,13,22]</sup>. This is similar to the CNV process of AMD patients<sup>[23]</sup>. As the parameters of laser can be accurately controlled, the CNV lesions of this model are consistent, moreover, it is also convenient to quantify the CNV by using choroidal flat mounts. Therefore, the laser-induced CNV model is considered as reliable and stable<sup>[12]</sup>. However, this model is not an ideal one as it created in healthy eyes and different from the situation in patient, for example, it does not include the oxidative stress factor. In our previous experiments, we induced CNV-like change in mice before injecting OxLDL into the subretinal space. As OxLDL is mainly deposited around RPE cells, OxLDL subretinal injection-induced CNV is more relevant to the real situation<sup>[7]</sup>. However, subretinal injection is more difficult to perform. Even if the trans-vitreous and trans-scleral approaches are adopted, bleeding, retinal detachment, complicated cataract, and other complications are more common<sup>[1]</sup>. In addition, the actual injected volume is inconsistent and the CNV area cannot be conveniently calculated.

Intravitreal injection is now widely used in ocular drug delivery, for example, anti-VEGF treatment for retinal and choroidal diseases<sup>[24]</sup>. In contrast to subretinal injection, intravitreal injection is much easier, shows better repeatability, and causes lower levels of damage. Based on above, we speculated whether intravitreal injection of OxLDL could promote the laser induced CNV in mice, thus creating a better model to study the detailed mechanism of OxLDL in wet-AMD.

We injected OxLDL into the vitreous after laser photocoagulation and found that the mean CNV area of the OxLDL injection group was significantly larger than that of LDL and PBS injection groups, suggesting that intravitreal injected OxLDL could promote the formation of laser-induced CNV. About the mechanism, we think that there may have two possibilities. One is that OxLDL spreads firstly through the laser-damaged retinas to the sub-retinal space and then stimulates the release of inflammatory and growth factors which further cause aggregation of inflammatory cells or promote angiogenesis. This possibility was confirmed by the finding that there had an increased content of OxPLs and macrophages surrounding CNV lesions<sup>[25-27]</sup>, and increased expression of IL-1 $\beta$ , IL-6, MMP9, and CCR2 in Choroid-RPE complex. Another possibility is that OxLDL in the vitreous stimulates the surrounding retinal cells to release cytokines and growth factors, which then diffuse through the retina to the subretinal cavity to exert their functions.

Similar to the results of our previous experiments, *in vitro* experiment with ARPE19 showed that OxLDL promotes the expression of IL-1 $\beta$ , IL-6, and VEGF, whereas LDL has no such effect. LOX1 is one of the main receptors of OxLDL, some of its effects were LOX1 dependent<sup>[28]</sup>. In our experiment, increased LOX1 expression was found in a dose-dependent manner when treated with OxLDL. In order to confirm whether LOX1 is involved in this process, we then inhibited LOX with its specific inhibitor and found that the expression of IL-1 $\beta$  and VEGF was decreased. This means that the effects of OxLDL on RPE cells are at least partly through LOX1<sup>[29]</sup>.

Different from *in vitro* results that LDL has no effect on the expression of IL-1 $\beta$ , IL-6, CCR2, and MMP9, *in vivo* experiment showed that expression of these factors in the choroidal tissue from the LDL group was increased when compared with that in the PBS group, although this increase was less than that in the OxLDL group. Considering the reason behind this, we speculated that the difference in LDL species might be the cause. The OxLDL and LDL we used were derived from the human serum, and this kind of LDL might induce some extent of immune response when injected into mouse vitreous, even in the absence of immune cells.

In summary, using intravitreal injection of OxLDL and laser

photocoagulation, we created a new CNV model. As this model involves both oxidative stress and Bruch's membrane damage, it is theoretically closer to the pathological changes of CNV in AMD patients. Furthermore, this method is relatively simple, shows good repeatability and the convenience for CNV quantification. Thus, this animal model is a simple and reliable one for studying the detailed mechanism of CNV formation and its interventions.

The shortcoming of our experiments is that we did not measure the cytokines and growth factors in vitreous, so we could not prove or exclude the second possibility that how OxLDL works when injected into the vitreous. Besides, the OxLDL is located beneath the retina in AMD patients, so this model we created is a trade-off between idealization and simplification, it is still not a perfect one.

#### ACKNOWLEDGEMENTS

**Foundations:** Supported by the National Natural Science Foundation of China (No.81470654); Science and Technology Plan of Natural Science Foundation of Shaanxi Province (No.2019SF-047).

**Conflicts of Interest:** Wu T, None; Dang KR, None; Wang YF, None; Lyu BZ, None; Xu WQ, None; Dou GR, None; Zhou J, None; Hui YN, None; Du HJ, None.

#### REFERENCES

- 1 Resnikoff S, Pascolini D, Etya'ale D, Kocur I, Pararajasegaram R, Pokharel GP, Mariotti SP. Global data on visual impairment in the year 2002. *Bull World Health Organ* 2004;82(11):844-851.
- 2 Freund KB, Yannuzzi LA, Sorenson JA. Age-related macular degeneration and choroidal neovascularization. *Am J Ophthalmol* 1993;115(6):786-791.
- 3 Velez-Montoya R, Oliver SC, Olson JL, Fine SL, Mandava N, Quiroz-Mercado H. Current knowledge and trends in age-related macular degeneration: today's and future treatments. *Retina* 2013;33(8):1487-1502.
- 4 Khan KN, Mahroo OA, Khan RS, Mohamed MD, McKibbin M, Bird A, Michaelides M, Tufail A, Moore AT. Differentiating drusen: Drusen and drusen-like appearances associated with ageing, age-related macular degeneration, inherited eye disease and other pathological processes. *Prog Retin Eye Res* 2016;53:70-106.
- 5 Yamada Y, Tian J, Yang YQ, Cutler RG, Wu TH, Telljohann RS, Mattson MP, Handa JT. Oxidized low density lipoproteins induce a pathologic response by retinal pigmented epithelial cells. *J Neurochem* 2008;105(4):1187-1197.
- 6 Picard E, Houssier M, Bujold K, *et al.* CD36 plays an important role in the clearance of oxLDL and associated age-dependent sub-retinal deposits. *Aging (Albany NY)* 2010;2(12):981-989.
- 7 Shaw PX, Zhang L, Zhang M, *et al.* Complement factor H genotypes impact risk of age-related macular degeneration by interaction with oxidized phospholipids. *Proc Natl Acad Sci U S A* 2012;109(34):13757-13762.

- 8 Lu ZG, Lin V, May A, Che B, Xiao X, Shaw DH, Su F, Wang ZH, Du HJ, Shaw PX. HTRA1 synergizes with oxidized phospholipids in promoting inflammation and macrophage infiltration essential for ocular VEGF expression. *PLoS One* 2019;14(5):e0216808.
- 9 Chou MY, Hartvigsen K, Hansen LF, Fogelstrand L, Shaw PX, Boullier A, Binder CJ, Witztum JL. Oxidation-specific epitopes are important targets of innate immunity. *J Intern Med* 2008;263(5):479-488.
- 10 Du HJ, Xiao X, Stiles T, Douglas C, Ho D, Shaw PX. Novel mechanistic interplay between products of oxidative stress and components of the complement system in AMD pathogenesis. *Open J Ophthalmol* 2016;6(1):43-50.
- 11 Miller H, Miller B, Ishibashi T, Ryan SJ. Pathogenesis of laser-induced choroidal subretinal neovascularization. *Invest Ophthalmol Vis Sci* 1990;31(5):899-908.
- 12 Shah RS, Soetikno BT, Lajko M, Fawzi AA. A mouse model for laser-induced choroidal neovascularization. *J Vis Exp* 2015(106):e53502.
- 13 Lambert V, Lecomte J, Hansen S, Blacher S, Gonzalez ML, Struman I, Sounni NE, Rozet E, de Tullio P, Foidart JM, Rakic JM, Noel A. Laser-induced choroidal neovascularization model to study age-related macular degeneration in mice. *Nat Protoc* 2013;8(11):2197-2211.
- 14 Shah SS, Denham LV, Elison JR, Bhattacharjee PS, Clement C, Huq T, Hill JM. Drug delivery to the posterior segment of the eye for pharmacologic therapy. *Expert Rev Ophthalmol* 2010;5(1):75-93.
- 15 Du HJ, Sun XF, Guma M, Luo J, Ouyang H, Zhang XH, Zeng J, Quach J, Nguyen DH, Shaw PX, Karin M, Zhang K. JNK inhibition reduces apoptosis and neovascularization in a murine model of age-related macular degeneration. *Proc Natl Acad Sci U S A* 2013;110(6):2377-2382.
- 16 Chen XP, Xun KL, Wu Q, Zhang TT, Shi JS, Du GH. Oxidized low density lipoprotein receptor-1 mediates oxidized low density lipoprotein-induced apoptosis in human umbilical vein endothelial cells: role of reactive oxygen species. *Vascul Pharmacol* 2007;47(1):1-9.
- 17 Hutter R, Speidl WS, Valdiviezo C, Sauter B, Corti R, Fuster V, Badimon JJ. Macrophages transmit potent proangiogenic effects of oxLDL *in vitro* and *in vivo* involving HIF-1 $\alpha$  activation: a novel aspect of angiogenesis in atherosclerosis. *J Cardiovasc Transl Res* 2013;6(4):558-569.
- 18 Wu T, Xu WQ, Wang YF, Tao MZ, Hu ZC, Lv B, Hui YN, Du HJ. OxLDL enhances choroidal neovascularization lesion through inducing vascular endothelium to mesenchymal transition process and angiogenic factor expression. *Cell Signal* 2020;70:109571.
- 19 Farhangkhoe H, Khan ZA, Barbin Y, Chakrabarti S. Glucose-induced up-regulation of CD36 mediates oxidative stress and microvascular endothelial cell dysfunction. *Diabetologia* 2005;48(7):1401-1410.
- 20 Yu JY, Du M, Elliott MH, Wu MY, Fu DX, Yang SH, Basu A, Gu XW, Ma JX, Aston CE, Lyons TJ. Extravascular modified lipoproteins: a role in the propagation of diabetic retinopathy in a mouse model of type 1 diabetes. *Diabetologia* 2016;59(9):2026-2035.
- 21 Ebrahimi KB, Fijalkowski N, Cano M, Handa JT. Decreased membrane complement regulators in the retinal pigmented epithelium contributes to age-related macular degeneration. *J Pathol* 2013;229(5):729-742.
- 22 Zhu YJ, Lu Q, Shen JK, Zhang L, Gao YS, Shen X, Xie B. Improvement and optimization of standards for a preclinical animal test model of laser induced choroidal neovascularization. *PLoS One* 2014;9(4):e94743.
- 23 Hernández-Zimbrón LF, Zamora-Alvarado R, Ochoa-De la Paz L, Velez-Montoya R, Zenteno E, Gullias-Cañizo R, Quiroz-Mercado H, Gonzalez-Salinas R. Age-related macular degeneration: new paradigms for treatment and management of AMD. *Oxid Med Cell Longev* 2018;2018:8374647.
- 24 Mehta H, Tufail A, Daien V, Lee AY, Nguyen V, Ozturk M, Barthelmes D, Gillies MC. Real-world outcomes in patients with neovascular age-related macular degeneration treated with intravitreal vascular endothelial growth factor inhibitors. *Prog Retin Eye Res* 2018;65:127-146.
- 25 Tian B, Al-Moujahed A, Bouzika P, Hu YJ, Notomi S, Tsoka P, Miller JW, Lin HJ, Vavvas DG. Atorvastatin promotes phagocytosis and attenuates pro-inflammatory response in human retinal pigment epithelial cells. *Sci Rep* 2017;7(1):2329.
- 26 Biswas L, Zhou XZ, Dhillon B, Graham A, Shu XH. Retinal pigment epithelium cholesterol efflux mediated by the 18 kDa translocator protein, TSPO, a potential target for treating age-related macular degeneration. *Hum Mol Genet* 2017;26(22):4327-4339.
- 27 Gnanaguru G, Choi AR, Amarnani D, D'Amore PA. Oxidized lipoprotein uptake through the CD36 receptor activates the NLRP3 inflammasome in human retinal pigment epithelial cells. *Invest Ophthalmol Vis Sci* 2016;57(11):4704-4712.
- 28 Chistiakov DA, Melnichenko AA, Myasoedova VA, Grechko AV, Orekhov AN. Mechanisms of foam cell formation in atherosclerosis. *J Mol Med* 2017;95(11):1153-1165.
- 29 Honjo M, Nakamura K, Yamashiro K, Kiryu J, Tanihara H, McEvoy LM, Honda Y, Butcher EC, Masaki T, Sawamura T. Lectin-like oxidized LDL receptor-1 is a cell-adhesion molecule involved in endotoxin-induced inflammation. *Proc Natl Acad Sci U S A* 2003;100(3):1274-1279.